

# What drives Fe depletion in calc-alkaline magma differentiation: Insights from Fe isotopes

De-Hong Du<sup>1</sup>, Ming Tang<sup>2</sup>, Weiqiang Li<sup>1</sup>, Suzanne Mahlburg Kay<sup>3</sup> and Xiao-Lei Wang<sup>1\*</sup>

<sup>1</sup>State Key Laboratory for Mineral Deposits Research, School of Earth Sciences and Engineering, Nanjing University, Nanjing 210023, China

<sup>2</sup>Key Laboratory of Orogenic Belt and Crustal Evolution, MOE; School of Earth and Space Sciences, Peking University, Beijing 100871, China

<sup>3</sup>Department of Earth and Atmospheric Sciences, Cornell University, Ithaca, New York 14850, USA

## ABSTRACT

The continental crust is strongly depleted in iron relative to mid-oceanic ridge basalt, broadly identical to the calc-alkaline magmas, suggesting that calc-alkaline differentiation is key to continent formation. However, it remains contentious as to what drives Fe depletion during magmatic differentiation in the crust. The two competing hypotheses for calc-alkaline differentiation—magnetite versus garnet ( $\pm$  amphibole) fractionation—predict contrasting Fe isotopic fractionation pathways in evolved melts because magnetite preferentially depletes ferric, isotopically heavy Fe whereas garnet ( $\pm$  amphibole) does the opposite. We report whole-rock Fe isotope data for two suites of igneous rocks from the central Andes, which represent magmas traversing normal and thickened arc crust, respectively. The magmas traversing thickened crust show a strong Fe depletion trend and consistently high  $\delta^{56}\text{Fe}$  values ( $0.14\% \pm 0.02\%$ , 1 standard deviation [SD]), while those traversing normal crust are less depleted in Fe and show variable  $\delta^{56}\text{Fe}$  values ( $0.10\% \pm 0.05\%$ , 1SD). The two Andean suites are both isotopically heavier than Mariana arc (Pacific Ocean) magmas that differentiate along tholeiitic (Fe-enriching) paths. These results confirm that garnet ( $\pm$  amphibole) fractionation/retention is the primary driver of Fe depletion in calc-alkaline magmas, and highlight a role for crustal thickening in generating calc-alkaline magmas.

## INTRODUCTION

Arc magmatism is thought to have played a central role in the formation of continental crust because of the compositional similarities between the continental crust and arc magmas (e.g., Rudnick and Gao, 2014). In such comparisons, one critical but frequently overlooked signature of the continental crust is its calc-alkaline trends marked by strong iron depletion. While some arcs show prominent calc-alkaline features (e.g., the central Andes), others, like the Mariana arc, are more tholeiitic, with significant Fe enrichment during early-stage differentiation, similar to the mid-ocean ridge trend (Fig. 1A).

The mechanism that drives Fe depletion in calc-alkaline differentiation remains debated. One explanation invokes early saturation of magnetite from arc magmas with high oxygen fugacity ( $f_{\text{O}_2}$ ) and  $\text{H}_2\text{O}$  contents (Osborn, 1959;

Sisson and Grove, 1993; Zimmer et al., 2010). However, continuous precipitation of  $\text{Fe}^{3+}$ -enriched magnetite will decrease the  $\text{Fe}^{3+}/\Sigma\text{Fe}$  of the residual melt whose  $f_{\text{O}_2}$  is not buffered. Such low  $\text{Fe}^{3+}/\Sigma\text{Fe}$  levels are not observed among arc magmas (Grocke et al., 2016), which implies that either magnetite is not a common fractionating phase or that these magmas evolved open to oxygen exchange. Moreover, the magnetite model cannot explain the preferential occurrence of calc-alkaline magmas in arcs with thick crust since high pressure would suppress magnetite saturation (Matjuschkin et al., 2016; Tang et al., 2019). Alternatively, fractionation and/or retention of garnet, a ferrous Fe-rich phase ( $\text{Fe}^{3+}/\Sigma\text{Fe} \leq 0.1$ ; Tang et al., 2019) that favors high pressure and  $\text{H}_2\text{O}$  content, could simultaneously drive Fe depletion and oxidation in arc magmas (Green and Ringwood, 1968; Alonso-Perez et al., 2009; Tang et al., 2018). Another  $\text{Fe}^{2+}$ -bearing mineral, amphibole, is also thought to have played an important role

in driving calc-alkaline magma differentiation (Kay et al., 1991; Kay and Mpodozis, 2001). These competing mechanisms for calc-alkaline differentiation have contrasting implications for continental crust formation.

Iron isotopes have the potential to resolve the mechanism for Fe depletion in calc-alkaline magmas. Inter-mineral Fe isotope fractionation arises because the smaller  $\text{Fe}^{3+}$  that prefers low coordination (IV-fold) tends to be associated with stiffer Fe-O bonds relative to the larger  $\text{Fe}^{2+}$ , and thus  $\text{Fe}^{3+}$  sites tend to enrich heavy Fe isotopes (e.g., Sossi and O'Neill, 2017). Therefore,  $\text{Fe}^{3+}$ -rich magnetite is expected to concentrate heavy Fe isotopes (Fig. 1B; Sossi et al., 2012; Dauphas et al., 2014; Roskosz et al., 2015), and its fractionation will drive the remaining melt toward lighter Fe isotope compositions (Fig. 1C). In contrast,  $\text{Fe}^{2+}$  in garnet is in VIII-fold coordination that is much higher than that of silicate melts (V-fold, on average) and other  $\text{Fe}^{2+}$ -bearing silicate minerals (VI-fold), implying that garnet enriches light Fe isotopes relative to other  $\text{Fe}^{2+}$ -bearing silicate minerals and melts (Fig. 1B; Dauphas et al., 2014; Sossi and O'Neill, 2017; Ye et al., 2020). Thus, garnet separation will lead to an enrichment of heavy Fe isotopes in the residual melts, which is opposite to the trend of magnetite fractionation (Fig. 1C). Amphibole has higher  $\text{Fe}^{3+}$  content ( $\text{Fe}^{3+}/\Sigma\text{Fe} \approx 0.25$ ) than garnet and tends to be slightly enriched in light Fe isotopes (Ye et al., 2020). Amphibole separation results in resolvable Fe isotope fractionation only when it removes over 85% of the total Fe (Fig. 1C).

We report Fe isotope data for two suites of magmatic rocks from the central Andes, a mature continental arc. These continental arc magma data are compared with those of the Mariana island arc, which allows us to evaluate

\*E-mail: [wxl@nju.edu.cn](mailto:wxl@nju.edu.cn)

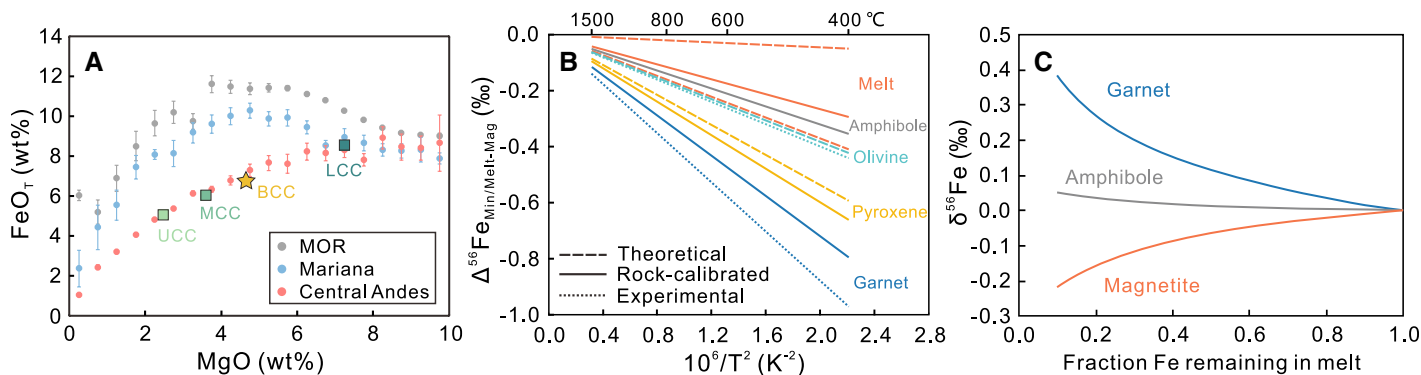


**Figure 1. (A) Average FeO<sub>T</sub>-MgO differentiation trends in arc and mid-ocean ridge (MOR) magmas. The data for the Mariana and central Andes arcs are from the GEOROC database (<http://georoc.mpch-mainz.gwdg.de/georoc/>), and MOR data are from Keller et al. (2015). The bulk continental crust (BCC), lower continental crust (LCC), middle continental crust (MCC), and upper continental crust (UCC) are from Rudnick and Gao (2014). (B) Compilation of published mineral/melt-magnetite fractionation factors for Fe isotopes (summarized in the Supplemental Material [see footnote 1]). Dashed, dotted, and solid lines represent theoretical, experimental, and rock-calibrated constraints, respectively. (C) Modeled  $\delta^{56}\text{Fe}$  of the evolving melt for specific mineral fractionation (at 900 °C) used a Rayleigh fractionation model based on the rock-calibrated fractionation factors.**

the Fe isotope systematics in different arcs and the mechanism for Fe depletion in calc-alkaline differentiation.

### GEOLOGICAL BACKGROUND AND SAMPLES

The Neogene Andean magmatic arc rocks analyzed here are from between 27°S and 29.3°S in the transition region between the modern southern Central Volcanic Zone arc (CVZ, ~22–28°S) and the currently inactive portion of the Andean arc over the Chilean-Pampean flat-slab (~28–33°S). The transect traverses the region over which the modern subduction angle of the Nazca plate beneath the South American backarc changes from ~30° in the north to nearly sub-horizontal in the south (Fig. 2; Mulcahy et al., 2014). The selected samples (33–3 Ma) are from the region of the Maricunga Belt arc and backarc west of the southernmost CVZ and its southward extension into the modern flat slab region under which the principal shallowing occurred after ca. 14–12 Ma (Kay and Mpodozis, 2002). The ca. 18–10 Ma samples are from magmas that erupted after the Andean margin went into compression and as the ~35–40-km-thick crust under the arc began thickening to reach ~55–60 km by ca. 12–10 Ma (Kay and Mpodozis, 2002; Kay et al., 2013; Heit et al., 2014). The ca. 9–3 Ma samples erupted as the Maricunga arc expanded ~50 km to the east at 8–3 Ma as the arc front was repositioned to the < 2 Ma CVZ (Goss et al., 2013).

The magmatic suite selected for Fe isotope analysis consists of 32 samples ranging from basaltic andesite to rhyolite, that all follow the calc-alkaline differentiation trend (Fig. 3A) and represent differentiation series generated before and after the most significant crustal thickening, which occurred by ca. 12–10 Ma. All are suggested to have been generated by the interaction of mantle-wedge-derived mafic arc magmas with continental crust (Kay et al.,

2013; Goss et al., 2013). The “Normal Crust” samples (>9 Ma) were selected from the Maricunga belt and Chilean-Pampean flat-slab region before and as the crust began thickening (Fig. 2). They are characterized by a moderate Fe-depletion differentiation trend (Fig. 3A) and low La/Yb (6–17) and Sm/Yb (2–3; Fig. 3B) ratios; these are consistent with extensive amphibole, but limited garnet, fractionation (Kay et al., 1991; Kay and Mpodozis, 2001). The “Thick

Crust” samples (<9 Ma) were selected from the southern CVZ region, which has thickened crust. They differ from the older suite in showing a strong Fe-depletion trend (Fig. 3A) and high La/Yb (17–63) and Sm/Yb ratios (3–9; Fig. 3B). They have been argued to be derived from the interaction of wedge-derived magmas with eclogitized lower crust and fore-arc crust that was incorporated into the mantle wedge during arc migration (Goss and Kay, 2009; Goss

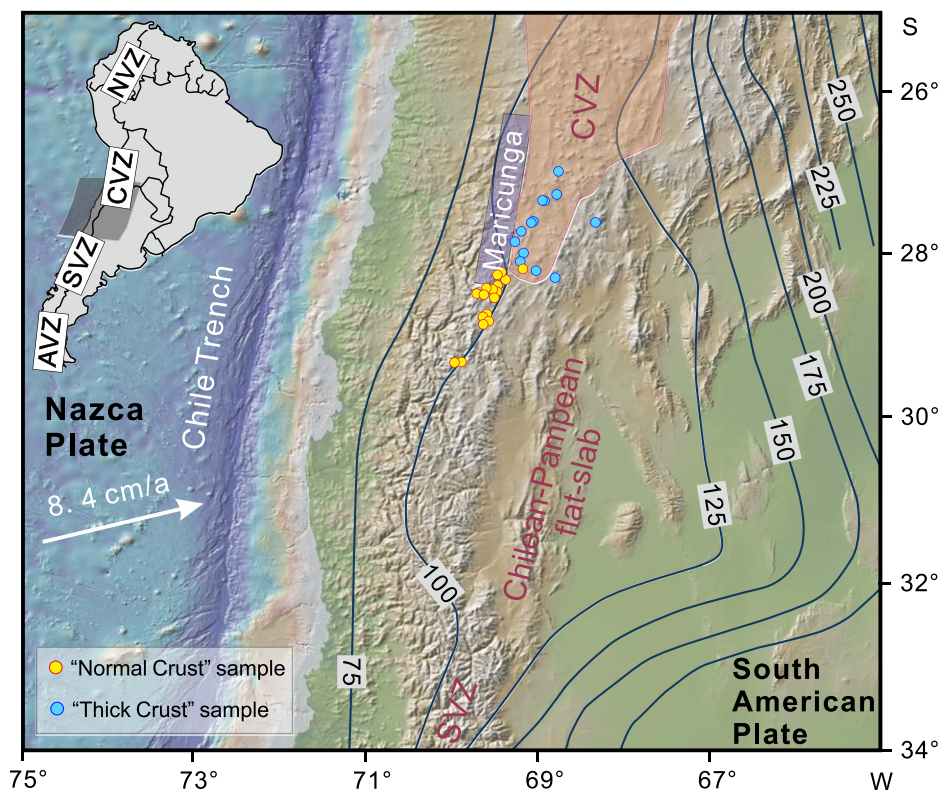


**Figure 2. Simplified geological map showing the main tectonic features of the central Andes (modified from Mulcahy et al., 2014). Solid lines represent depth contours (in km) of the subducting Nazca plate across the Wadati-Benioff zone. The base map was generated using the GeoMapApp software (<http://www.geomapp.org/>). AVZ—Austral volcanic zone; SVZ—southern volcanic zone; CVZ—central volcanic zone; NVZ—northern volcanic zone.**

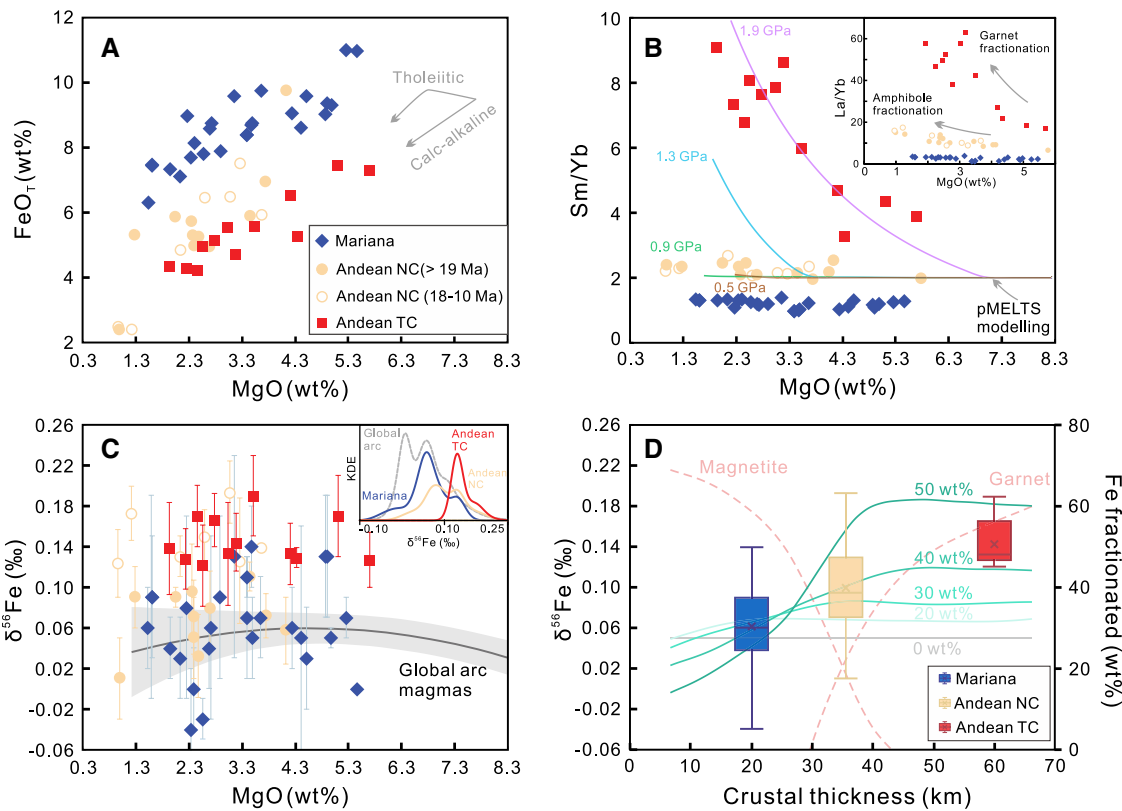


**Figure 3.** Diagrams showing (A)  $\text{FeO}_T$  (T-total) contents, (B) Sm/Yb (and La/Yb) ratios, and (C,D)  $\delta^{56}\text{Fe}$  values of the arc magmas from thin arc crust (Mariana arc), normal crust (Andean NC), and thick crust (Andean TC). For pMELTS software, see Ghorso et al. (2002). Fe isotope data of the Mariana arc are from Williams et al. (2018). Inset in (C) shows Kernel density estimate (KDE) of the  $\delta^{56}\text{Fe}$  for arc magmas from different arcs. Gray shaded areas in C represent the trend of global arc magmas (Foden et al., 2018). Dashed lines in D represent the iron fraction of magnetite/garnet to the bulk cumulate after 50 wt% crystallization. Solid lines in D are magma  $\delta^{56}\text{Fe}$  evolution paths from 0 wt% to 50 wt% crystallinity. The initial arc melt is assumed to have a  $\delta^{56}\text{Fe}$  value of 0.05‰ (Foden et al., 2018).

et al., 2013). Irrespective of the exact genesis of the “Thick Crust” magmas, these magmas had equilibrated with garnet during differentiation in the garnet stability field of the thickened crust.

More detailed petrography and geochemistry of most of the samples can be found in Goss et al. (2013) and Goss and Kay (2009) and references therein. The analytical methods and Fe isotope data are presented in the Supplemental Material<sup>1</sup>.

## RESULTS

The Andean “Thick Crust” samples exhibit a small variation in  $\delta^{56}\text{Fe}$  values (Figs. 3C and 3D) ranging from  $0.12\text{‰} \pm 0.04\text{‰}$  to  $0.19\text{‰} \pm 0.04\text{‰}$  (2 SD), with a mean of  $0.14\text{‰} \pm 0.02\text{‰}$  (1 SD). The values are slightly higher than those of mid-oceanic ridge basalt (MORB) ( $\delta^{56}\text{Fe} = 0.103\text{‰} \pm 0.035\text{‰}$ , 1 SD; Johnson et al., 2020) and significantly higher than those of average mafic arc magmas that differentiated within thin-normal arc crusts (tholeiitic and transitional calc-alkaline,  $\delta^{56}\text{Fe} = 0.050\text{‰} \pm 0.025\text{‰}$ , 1SD; Foden et al., 2018). Compared with the “Thick Crust” samples, the “Normal Crust” samples show a larger dispersion in  $\delta^{56}\text{Fe}$  (Fig. 3C), from  $0.01\text{‰} \pm 0.04\text{‰}$

to  $0.19\text{‰} \pm 0.03\text{‰}$  (2 SD), with a mean of  $0.10\text{‰} \pm 0.05\text{‰}$  (1 SD). Specifically, the older “Normal Crust” samples (>19 Ma) have lower  $\delta^{56}\text{Fe}$  values ( $0.01\text{‰}$ – $0.11\text{‰}$ ; Fig. 3C), while the younger “Normal Crust” samples (18–10 Ma) have higher  $\delta^{56}\text{Fe}$  values ( $0.12\text{‰}$ – $0.19\text{‰}$ ; Fig. 3C). Both Andean suites have  $\delta^{56}\text{Fe}$  values that are higher than those of the Mariana arc magmas (mean  $\delta^{56}\text{Fe} = 0.06\text{‰} \pm 0.05\text{‰}$ , 1 SD; Williams et al., 2018), which differentiated within a thin arc crust (~20 km; Takahashi et al., 2007) following a tholeiitic trend. Although there is no evident correlation between  $\delta^{56}\text{Fe}$  and Sm/Yb and MgO (Fig. 3C),  $\delta^{56}\text{Fe}$  of arc magmas generally tends to increase with crustal thickness (Fig. 3D), and the  $\delta^{56}\text{Fe}$  values of the Andean suites are similar to the estimated  $\delta^{56}\text{Fe}$  values of the upper continental crust (~0.1‰; Johnson et al., 2020).

## DISCUSSION

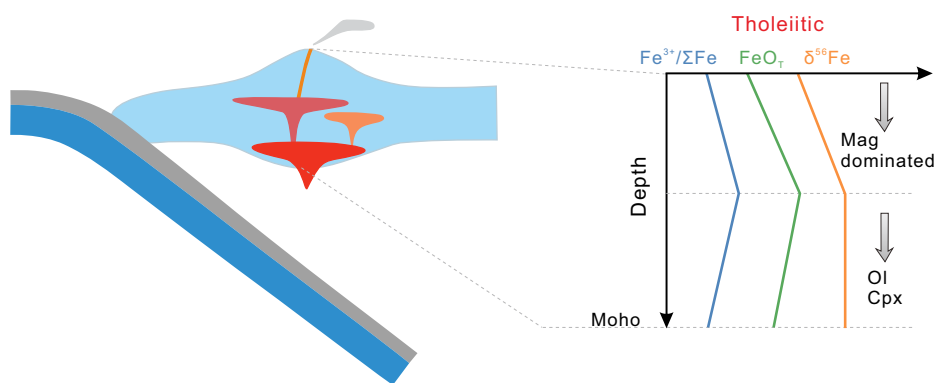
Iron isotope variability in arc magmas may be caused by several processes, including (1) fluid addition in the mantle wedge, (2) peridotite partial melting, (3) source heterogeneity, and (4) intracrustal differentiation. Slab-derived fluids may introduce light Fe isotopes into arc magmas (e.g., Debret et al., 2016). However, Andean magmas have higher  $\delta^{56}\text{Fe}$  values than other arc magmas and MORBs, and there are no clear covariations of  $\delta^{56}\text{Fe}$  with geochemical tracers of fluid activity (e.g., Ba/La ratio), which indicates the limited contribution of fluid addition to the Fe isotope variations of Andean magmas.

Iron isotopes may be fractionated during mantle partial melting such that melts are preferentially enriched in heavy Fe isotopes (Weyer and Ionov, 2007; Dauphas et al., 2014), and the extraction of such melts can shift the source toward lower  $\delta^{56}\text{Fe}$  (Weyer and Ionov, 2007). Although mantle sources are likely heterogeneous, a global survey of Fe isotopes in mafic arc magmas by Foden et al. (2018) shows that primitive arc magmas (mean  $\delta^{56}\text{Fe} = 0.050\text{‰} \pm 0.025\text{‰}$ , 1 SD) derived by the partial melting of mantle wedge sources ( $\delta^{56}\text{Fe}$  of ~0.025‰) are systematically lighter than the evolved Andean arc magmas studied here (Fig. 3C). These observations suggest that melting-induced fractionation is unlikely to explain the elevated  $\delta^{56}\text{Fe}$  values of the Andean arc magmas.

The increasing magma  $\delta^{56}\text{Fe}$  with crustal thickening (Fig. 3D) implies a first-order control of pressure on Fe isotope fractionation during arc magma differentiation. The Andean and Mariana suites have comparable MgO contents (Fig. 3), which suggests similar degrees of differentiation. The systematically elevated  $\delta^{56}\text{Fe}$  and high Sm/Yb in the Andean “Thick Crust” suite (Figs. 3B and 3C) are consistent with the retention of Fe in garnet ( $\pm$  amphibole) rather than magnetite fractionation. But the  $\delta^{56}\text{Fe}$ -MgO (and Sm/Yb) correlations may be obscured by the complex crystallizing/mixing processes in the shallow magma plumbing systems. In particular, amphibole separation can drive evident Fe

<sup>1</sup>Supplemental Material. Methods, supplemental figures, and data. Please visit <https://doi.org/10.1130/GEOL.S.18819686> to access the supplemental material, and contact [editing@geosociety.org](mailto:editing@geosociety.org) with any questions.

## A Thin island/continental arc



## B Thick continental arc

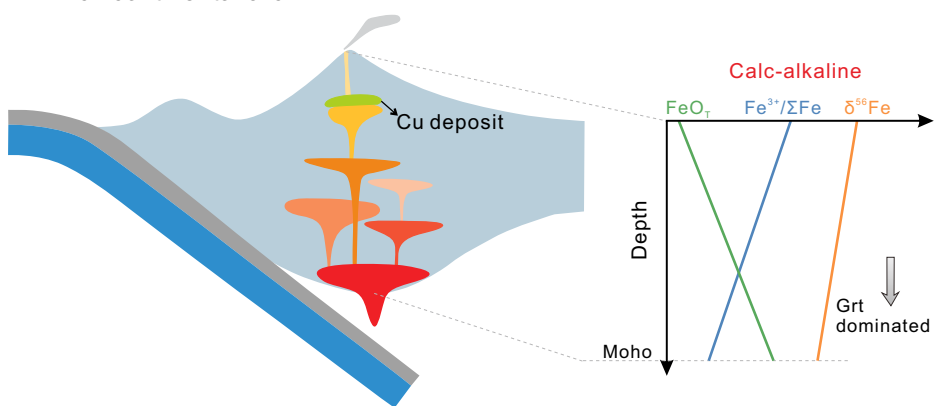


**Figure 4. Cartoon showing magma differentiation in (A) thin arc crust versus (B) thick arc crust, and schematic  $\text{FeO}_T$  (T—total),  $\text{Fe}^{3+}/\Sigma\text{Fe}$ , and  $\delta^{56}\text{Fe}$  profiles of arc magma differentiation. Mag—magnetite; Ol—olivine; Cpx—clinopyroxene; Cu—copper; Grt—garnet.**

and Mg depletions, but it has a limited effect on Sm/Yb in the evolving melts because amphibole-melt  $\text{KD}_{\text{Sm/Yb}}$  is  $\sim 1$  ( $\text{KD}$ —partition coefficient) (Adam and Green, 2006). Combined garnet and amphibole fractionations may thus weaken the correlation between  $\delta^{56}\text{Fe}$  and MgO (and Sm/Yb). In contrast, samples from the Mariana arc with  $\text{MgO} < 4 \text{ wt}\%$ , where the crust is much thinner, show systematically lighter Fe isotope signatures, which was explained by extensive magnetite fractionation (Williams et al., 2018). The Andean “Normal Crust” suite, with variable but intermediate average  $\delta^{56}\text{Fe}$ , represents a transitional calc-alkaline series dominated by amphibole ( $\pm$  magnetite) fractionation (Kay et al., 1991; Kay and Mpodozis, 2001).

To further illustrate the effect of crustal thickness on Fe isotope fractionation, we use pMELTS software (Ghiorso et al., 2002) to simulate arc magma differentiation under 0.2–2.0 GPa and 3 wt% initial  $\text{H}_2\text{O}$  content. We started with a primitive arc magma composition, and all simulations were buffered at QFM + 1. Simulations performed with other values of  $f_{\text{O}_2}$  are shown in the Supplemental Material. Amphibole was not evaluated since the current MELTS family software cannot predict amphibole sat-

uration effectively (Ghiorso et al., 2002). As shown in Figure 3D, magnetite is the dominant Fe-bearing phase when arc magmas differentiate within thin crust ( $< 30 \text{ km}$ ), whereas garnet is the major Fe-controlling phase in thick crust ( $> 45 \text{ km}$ ). Arc magmas differentiating in crust of intermediate thicknesses ( $\sim 30\text{--}45 \text{ km}$ ) may undergo garnet, amphibole, and magnetite fractionation. The modeled arc magma  $\delta^{56}\text{Fe}$  gradually increases with increasing crustal thickness as differentiation proceeds, consistent with the Fe isotope compositions of the Andean and Mariana arc samples. We recognize that the model here is highly simplified, but this semiquantitative approach allows us to evaluate the relative importance of garnet ( $\pm$  amphibole) and magnetite in the generation of calc-alkaline rock series.

Finally, one enigmatic observation comes from the younger “Normal Crust” samples (18–10 Ma), which have higher  $\delta^{56}\text{Fe}$  values but low Sm/Yb ratios. Amphibole fractionation alone cannot produce the high  $\delta^{56}\text{Fe}$  values of the younger “Normal Crust” samples. Instead, the observed  $\delta^{56}\text{Fe}$  values may reflect contributions from some isotopically heavy materials, such as a metasomatized mantle source (Weyer and Ionov, 2007).

## CONCLUSIONS AND IMPLICATIONS

Our findings highlight the pressure control on magma Fe isotope fractionation during arc magma differentiation. In particular, the systematically heavier Fe isotopes of the Andean “Thick Crust” suite as compared with those of the Mariana arc magmas point to garnet ( $\pm$  amphibole) fractionation/retention as the primary mechanism driving calc-alkaline series differentiation (Fig. 4). These observations have important implications for the formation of calc-alkaline continental crust. Although the continental crust is originally derived from the mantle, its Fe-depleted and Si-enriched bulk composition (andesitic) differs significantly from that of basaltic, mantle-derived magmas (e.g., Rudnick, 1995). Resolving this paradox requires removal of materials complementary to the andesitic continental crust. Our observations suggest that fractionation/retention of garnet ( $\pm$  amphibole)-bearing cumulates/residues from primitive arc magmas in thickened arc crust produces the magmas with strong Fe depletion and elevated  $\delta^{56}\text{Fe}$ , which are similar to those of the calc-alkaline continental crust (Fig. 3). These deep-seated cumulates/residues are denser than the underlying mantle due to abundant garnet and could founder back into the mantle (Kay and Kay, 1993; Jagoutz and Behn, 2013). Thus, fractionation and/or retention and subsequent foundering of deep-seated cumulates and/or residues form a missing link between the Fe-depleted andesitic continental crust and its basaltic precursor. This implies that synmagmatic crustal thickening is critical for making the calc-alkaline continental crust (Fig. 4).

## ACKNOWLEDGMENTS

This work was financially supported by the National Natural Science Foundation of China (grant 42025202 to X.-L. Wang; grant 41622301 to W. Li) and State Key Laboratory for Mineral Deposits Research (to M. Tang). We thank Paolo Sossi, Stefan Weyer, and an anonymous reviewer for their thoughtful comments, and editor Urs Schaltegger for efficient handling.

## REFERENCES CITED

- Adam, J., and Green, T., 2006, Trace element partitioning between mica and amphibole-bearing garnet lherzolite and hydrous basaltic melt: 1. Experimental results and the investigation of controls on partitioning behavior: *Contributions to Mineralogy and Petrology*, v. 152, p. 1–17, <https://doi.org/10.1007/s00410-006-0085-4>.
- Alonso-Perez, R., Müntener, O., and Ulmer, P., 2009, Igneous garnet and amphibole fractionation in the roots of island arcs: Experimental constraints on andesitic liquids: *Contributions to Mineralogy and Petrology*, v. 157, p. 541–558, <https://doi.org/10.1007/s00410-008-0351-8>.
- Dauphas, N., Roskosz, M., Alp, E.E., Neuville, D.R., Hu, M.Y., Sio, C.K., Tissot, F.L.H., Zhao, J., Tissandier, L., Médard, E., and Cordier, C., 2014, Magma redox and structural controls on iron isotope variations in Earth’s mantle and crust: *Earth and Planetary Science Letters*, v. 398, p. 127–140, <https://doi.org/10.1016/j.epsl.2014.04.033>.
- Debret, B., Millet, M.A., Pons, M.L., Bouilhol, P., Inglis, E., and Williams, H., 2016, Isotopic

- evidence for iron mobility during subduction: *Geology*, v. 44, p. 215–218, <https://doi.org/10.1130/G37565.1>.
- Foden, J., Sossi, P.A., and Nebel, O., 2018, Controls on the iron isotopic composition of global arc magmas: *Earth and Planetary Science Letters*, v. 494, p. 190–201, <https://doi.org/10.1016/j.epsl.2018.04.039>.
- Ghiorso, M.S., Hirschmann, M.M., Reiners, P.W., and Kress, V.C., III, 2002, The pMELTS: A revision of MELTS for improved calculation of phase relations and major element partitioning related to partial melting of the mantle to 3 GPa: *Geochemistry Geophysics Geosystems*, v. 3, p. 1–35, <https://doi.org/10.1029/2001GC000217>.
- Goss, A.R., and Kay, S.M., 2009, Extreme high field strength element (HFSE) depletion and near-chondritic Nb/Ta ratios in Central Andean adakite-like lavas (~28°S, ~68°W): *Earth and Planetary Science Letters*, v. 279, p. 97–109, <https://doi.org/10.1016/j.epsl.2008.12.035>.
- Goss, A.R., Kay, S.M., and Mpodozis, C., 2013, Andean adakites from the northern edge of the Chilean–Pampean flat-slab (27–28.5°S) associated with frontal arc migration and forearc subduction erosion: *Journal of Petrology*, v. 54, p. 2193–2234, <https://doi.org/10.1093/petrology/egt044>.
- Green, T.H., and Ringwood, A.E., 1968, Genesis of the calc-alkaline igneous rock suite: *Contributions to Mineralogy and Petrology*, v. 18, p. 105–162, <https://doi.org/10.1007/BF00371806>.
- Groce, S.B., Cottrell, E., de Silva, S., and Kelley, K.A., 2016, The role of crustal and eruptive processes versus source variations in controlling the oxidation state of iron in Central Andean magmas: *Earth and Planetary Science Letters*, v. 440, p. 92–104, <https://doi.org/10.1016/j.epsl.2016.01.026>.
- Heit, B., Bianchi, M., Yuan, X., Kay, S.M., Sandvol, E., Kumar, P., Kind, R., Alonso, R.N., Brown, L.D., and Comte, D., 2014, Structure of the crust and the lithosphere beneath the southern Puna plateau from teleseismic receiver functions: *Earth and Planetary Science Letters*, v. 385, p. 1–11, <https://doi.org/10.1016/j.epsl.2013.10.017>.
- Jagoutz, O., and Behn, M.D., 2013, Foundering of lower island-arc crust as an explanation for the origin of the continental Moho: *Nature*, v. 504, p. 131–134, <https://doi.org/10.1038/nature12758>.
- Johnson, C., Beard, B., and Weyer, S., 2020, High-temperature Fe isotope geochemistry, *in* Johnson, C., Beard, B., and Weyer, S., eds., *Iron Geochemistry: An Isotopic Perspective: Advances in Isotope Geochemistry*: Cham, Switzerland, Springer, p. 85–147, [https://doi.org/10.1007/978-3-030-33828-2\\_4](https://doi.org/10.1007/978-3-030-33828-2_4).
- Kay, R.W., and Kay, S.M., 1993, Delamination and delamination magmatism: *Tectonophysics*, v. 219, p. 177–189, [https://doi.org/10.1016/0040-1951\(93\)90295-U](https://doi.org/10.1016/0040-1951(93)90295-U).
- Kay, S.M., and Mpodozis, C., 2001, Central Andean ore deposits linked to evolving shallow subduction systems and thickening crust: *GSA Today*, v. 11, p. 4–9, [https://doi.org/10.1130/1052-5173\(2001\)011<0004:CAODLT>2.0.CO;2](https://doi.org/10.1130/1052-5173(2001)011<0004:CAODLT>2.0.CO;2).
- Kay, S.M., and Mpodozis, C., 2002, Magmatism as a probe to the Neogene shallowing of the Nazca plate beneath the modern Chilean flat-slab: *Journal of South American Earth Sciences*, v. 15, p. 39–57, [https://doi.org/10.1016/S0895-9811\(02\)00005-6](https://doi.org/10.1016/S0895-9811(02)00005-6).
- Kay, S.M., Mpodozis, C., Ramos, V.A., and Munizaga, F., 1991, Magma source variations for mid–late Tertiary magmatic rocks associated with a shallowing subduction zone and a thickening crust in the central Andes (28 to 33°S), *in* Harmon, R.S., and Rapela, C.W., *Andean Magmatism and Its Tectonic Setting*: Geological Society of America Special Paper 265, p. 113–138, <https://doi.org/10.1130/SPE265-p113>.
- Kay, S.M., Mpodozis, C., and Gardeweg, M., 2013, Magma sources and tectonic setting of Central Andean andesites (25.5–28°S) related to crustal thickening, forearc subduction erosion and delamination, *in* Gómez-Tuena, A., Straub, S.M., and Zeller, G.F., eds., *Orogenic Andesites and Crustal Growth*: Geological Society [London] Special Publication 385, p. 303–334, <https://doi.org/10.1144/SP385.11>.
- Keller, C.B., Schoene, B., Barboni, M., Samperton, K.M., and Husson, J.M., 2015, Volcanic–plutonic parity and the differentiation of the continental crust: *Nature*, v. 523, p. 301–307, <https://doi.org/10.1038/nature14584>.
- Matjuschkin, V., Blundy, J.D., and Brooker, R.A., 2016, The effect of pressure on sulphur speciation in mid- to deep-crustal arc magmas and implications for the formation of porphyry copper deposits: *Contributions to Mineralogy and Petrology*, v. 171, p. 66, <https://doi.org/10.1007/s00410-016-1274-4>.
- Mulcahy, P., Chen, C., Kay, S.M., Brown, L.D., Isacks, B.L., Sandvol, E., Heit, B., Yuan, X.H., and Coira, B.L., 2014, Central Andean mantle and crustal seismicity beneath the southern Puna plateau and the northern margin of the Chilean–Pampean slab: *Tectonics*, v. 33, p. 1636–1658, <https://doi.org/10.1002/2013TC003393>.
- Osborn, E.F., 1959, Role of oxygen pressure in the crystallization and differentiation of basaltic magma: *American Journal of Science*, v. 257, p. 609–647, <https://doi.org/10.2475/ajs.257.9.609>.
- Roskosz, M., Sio, C.K.I., Dauphas, N., Bi, W., Tissot, F.L.H., Hu, M.Y., Zhao, J., and Alp, E.E., 2015, Spinel–olivine–pyroxene equilibrium iron isotopic fractionation and applications to natural peridotites: *Geochimica et Cosmochimica Acta*, v. 169, p. 184–199, <https://doi.org/10.1016/j.gca.2015.07.035>.
- Rudnick, R.L., 1995, Making continental crust: *Nature*, v. 378, p. 571–578, <https://doi.org/10.1038/378571a0>.
- Rudnick, R.L., and Gao, S., 2014, Composition of the continental crust, *in* Rudnick, R.L., ed., *The Crust* (2nd edition), Volume 4: *Treatise on Geochemistry*: Oxford, UK, Elsevier, p. 1–51, <https://doi.org/10.1016/B978-0-08-095975-7.00301-6>.
- Sisson, T., and Grove, T., 1993, Experimental investigations of the role of H<sub>2</sub>O in calc-alkaline differentiation and subduction zone magmatism: *Contributions to Mineralogy and Petrology*, v. 113, p. 143–166, <https://doi.org/10.1007/BF00283225>.
- Sossi, P.A., and O'Neill, H.S.C., 2017, The effect of bonding environment on iron isotope fractionation between minerals at high temperature: *Geochimica et Cosmochimica Acta*, v. 196, p. 121–143, <https://doi.org/10.1016/j.gca.2016.09.017>.
- Sossi, P.A., Foden, J.D., and Halverson, G.P., 2012, Redox-controlled iron isotope fractionation during magmatic differentiation: An example from the Red Hill intrusion, S. Tasmania: *Contributions to Mineralogy and Petrology*, v. 164, p. 757–772, <https://doi.org/10.1007/s00410-012-0769-x>.
- Takahashi, N., Kodaira, S., Klemperer, S.L., Tatsumi, Y., Kaneda, Y., and Suyehiro, K., 2007, Crustal structure and evolution of the Mariana intra-oceanic island arc: *Geology*, v. 35, p. 203–206, <https://doi.org/10.1130/G23212A.1>.
- Tang, M., Erdman, M., Eldridge, G., and Lee, C.-T.A., 2018, The redox “filter” beneath magmatic orogens and the formation of continental crust: *Science Advances*, v. 4, eaar4444, <https://doi.org/10.1126/sciadv.aar4444>.
- Tang, M., Lee, C.-T.A., Costin, G., and Höfer, H.E., 2019, Recycling reduced iron at the base of magmatic orogens: *Earth and Planetary Science Letters*, v. 528, 115827, <https://doi.org/10.1016/j.epsl.2019.115827>.
- Weyer, S., and Ionov, D.A., 2007, Partial melting and melt percolation in the mantle: The message from Fe isotopes: *Earth and Planetary Science Letters*, v. 259, p. 119–133, <https://doi.org/10.1016/j.epsl.2007.04.033>.
- Williams, H.M., Prytulak, J., Woodhead, J.D., Kelley, K.A., Brounce, M., and Plank, T., 2018, Interplay of crystal fractionation, sulfide saturation and oxygen fugacity on the iron isotope composition of arc lavas: An example from the Marianas: *Geochimica et Cosmochimica Acta*, v. 226, p. 224–243, <https://doi.org/10.1016/j.gca.2018.02.008>.
- Ye, H., Wu, C., Brzozowski, M.J., Yang, T., Zha, X., Zhao, S., Gao, B., and Li, W., 2020, Calibrating equilibrium Fe isotope fractionation factors between magnetite, garnet, amphibole, and biotite: *Geochimica et Cosmochimica Acta*, v. 271, p. 78–95, <https://doi.org/10.1016/j.gca.2019.12.014>.
- Zimmer, M.M., Plank, T., Hauri, E.H., Yagodinski, G.M., Stelling, P., Larsen, J., Singer, B., Jicha, B., Mandeville, C., and Nye, C.J., 2010, The role of water in generating the calc-alkaline trend: New volatile data for Aleutian magmas and a new tholeiitic index: *Journal of Petrology*, v. 51, p. 2411–2444, <https://doi.org/10.1093/petrology/egq062>.

Printed in USA